WEEK 21

8.12 Jiameng Nie

Gene knockout

We used colony PCR to verify *tyrR* knockout (3_{rd} time) (based on BL21*ΔtyrB*) (Figure 1). We tested the transform efficiency of BL21*ΔtyrB* competent cells and found that the efficiency is low (Figure 2, 3). Therefore, we re-prepared BL21*ΔtyrB* eletrocompetent cells and optimized the electroporation method and eletrocompetent cells preparation method. At the same time, we prepared BL21*ΔtyrR* chemical competent cells (Figure 5) and pTarget-aspC (Figure 6, 7).

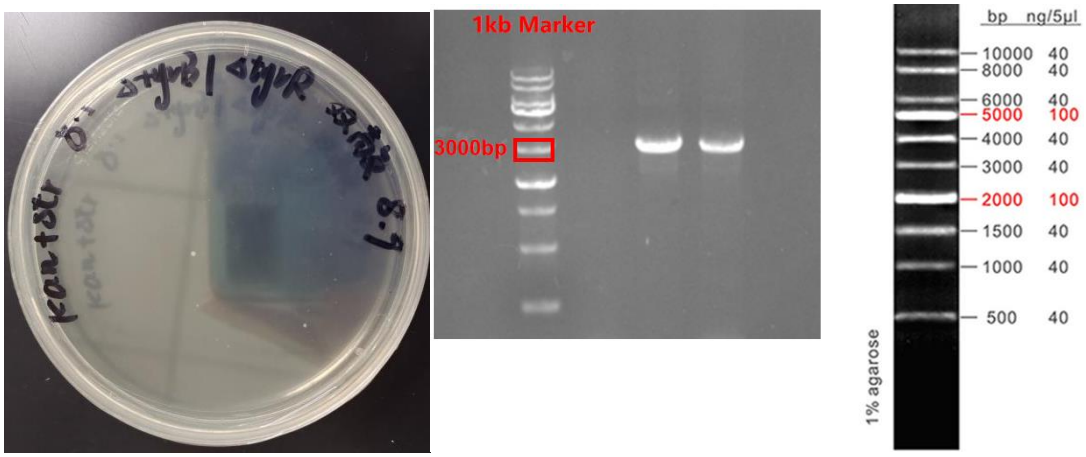

Figure 1 The result of *tyrR* knockout (3_{rd} time)

Choose 2 clones to have colony PCR. No correct band (1400 bp) was shown.

2.5 pg pUC 19 DNA was mixed with 25 μL electrocompetent cells to test the efficiency.

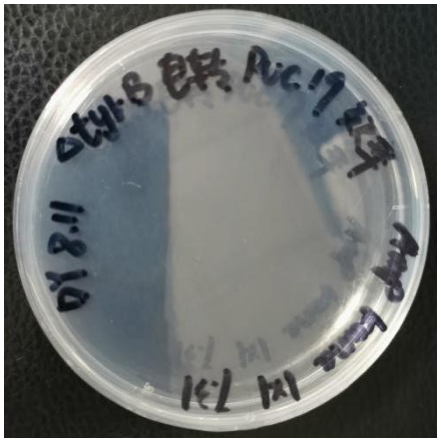

Figure 2 Use pUC 19 to test the efficiency of BL21*ΔtyrB* eletrocompetent cells

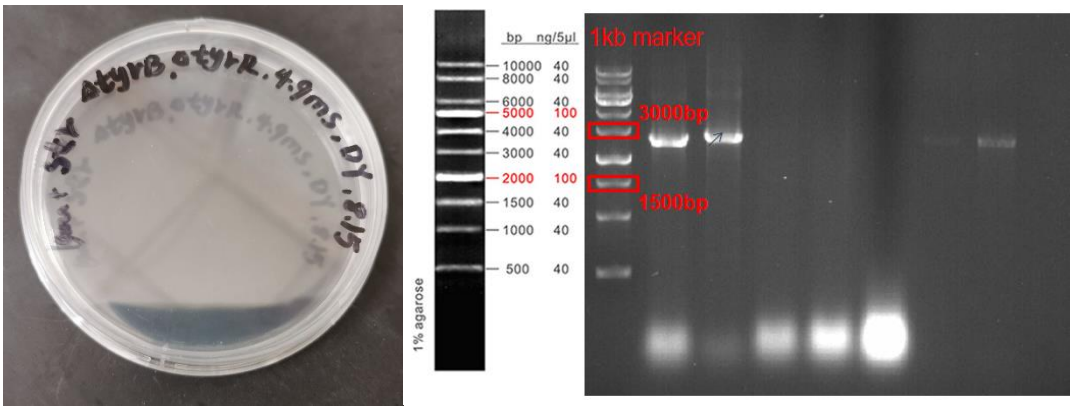

Figure 3 Used BL21*ΔtyrB* eletrocompetent cells to knock *aspC* out, colony PCR were used to verify the knockout

No correct band was shown in electrophoresis. Because of the low electroporation efficiency of BL21*ΔtyrB* competent cells, we optimized the eletrocompetent cell preparation method and re-prepared the BL21*ΔtyrB* eletrocompetent cells.

Our preparation method is shown on protocols.io

(DOI: dx.doi.org/10.17504/protocols.io.byuxpwxn)

940 pg pUAM was mixed with 25 μL electrocompetent cells to test the efficiency.

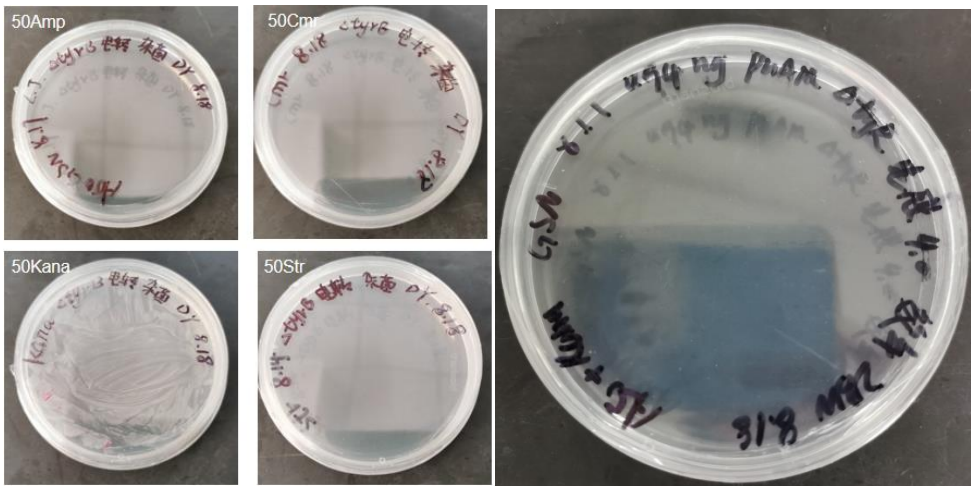

Figure 4 Pollution detection and efficiency test of BL21*ΔtyrB* eletrocompetent cells, left, pollution detection; right, efficiency test

8 clones were shown on the plate after culture at 30 ℃ for 20 h. The efficiency was still low, therefore, the reason still needed to be analyzed.

5 pg pUC 19 was mixed with 100 μL competent cells to test the efficiency.

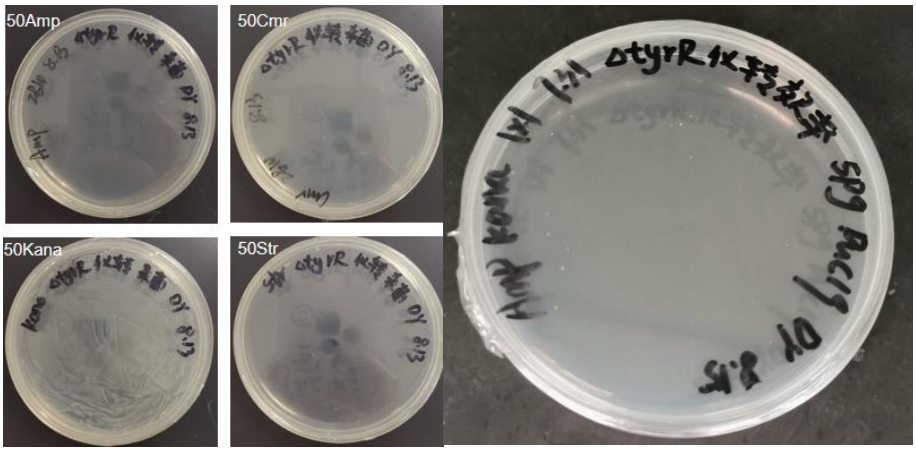

Figure 5 Pollution detection and efficiency test of BL21*ΔtyrR* chemical competent cells, left, pollution detection; right, efficiency test

11 clones were shown on the plate after culture at 37 ℃ for 20 h. Therefore, the transformation efficiency of BL21*ΔtyrR* chemical competent cells is low. But the low cell quantity may also caused by the loss of Pcas9 plasmid. Therefore, further test was needed.

Reaction system & progress (10μL)	
Dpn I	0.2μL
cutsmart	1μL
pTarget-613	1μL
ddw	22μL
37℃	2h
70℃	10min

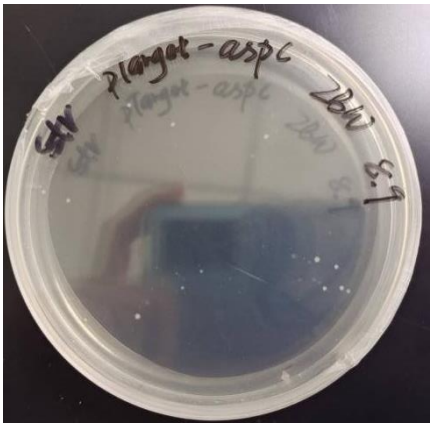

Figure 6 Left, DpnI digestion system and progress; right, transformed 10 μL digestion product into 50 μL T1 chemical competent cells and plated on LB medium with streptomycin

Figure 7 Sequencing of pTarget-aspC

DNA sequencing correct.

8.13 Shuhan Liu

Gradient HMA concentration induction assay & fluorescence re-screening

We used gradient HMA concentration induction assay to further study the operational range of F5-B7.

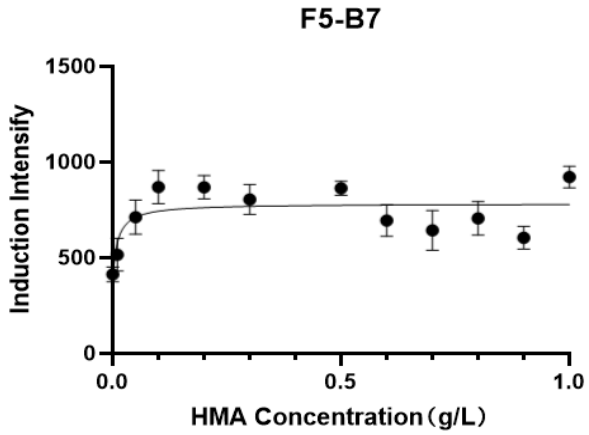

Figure 8 Gradient HMA concentration induction assay of F5-B7

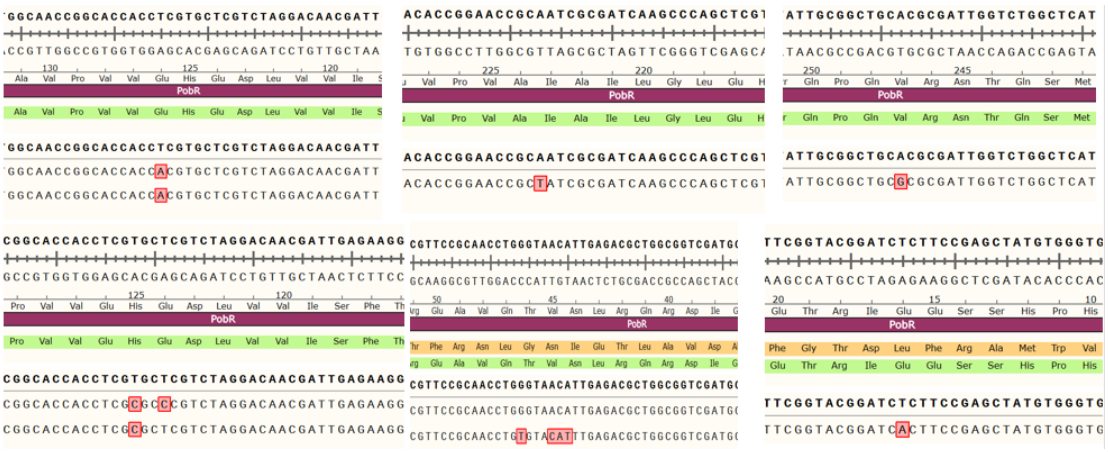

Figure 9 Sequencing of the subclone of F5-B7, above, subclone C9; below, subclone C7

Pollution were found in the culture of F5-B7. Therefore, we used streak plate method to isolated monoclones of 10 clones with the highest ratio of IA/I0 in re-screening last time. Picked 3 monoclones of each clone in 10 clones on the plate to have fluorescence re-screening.

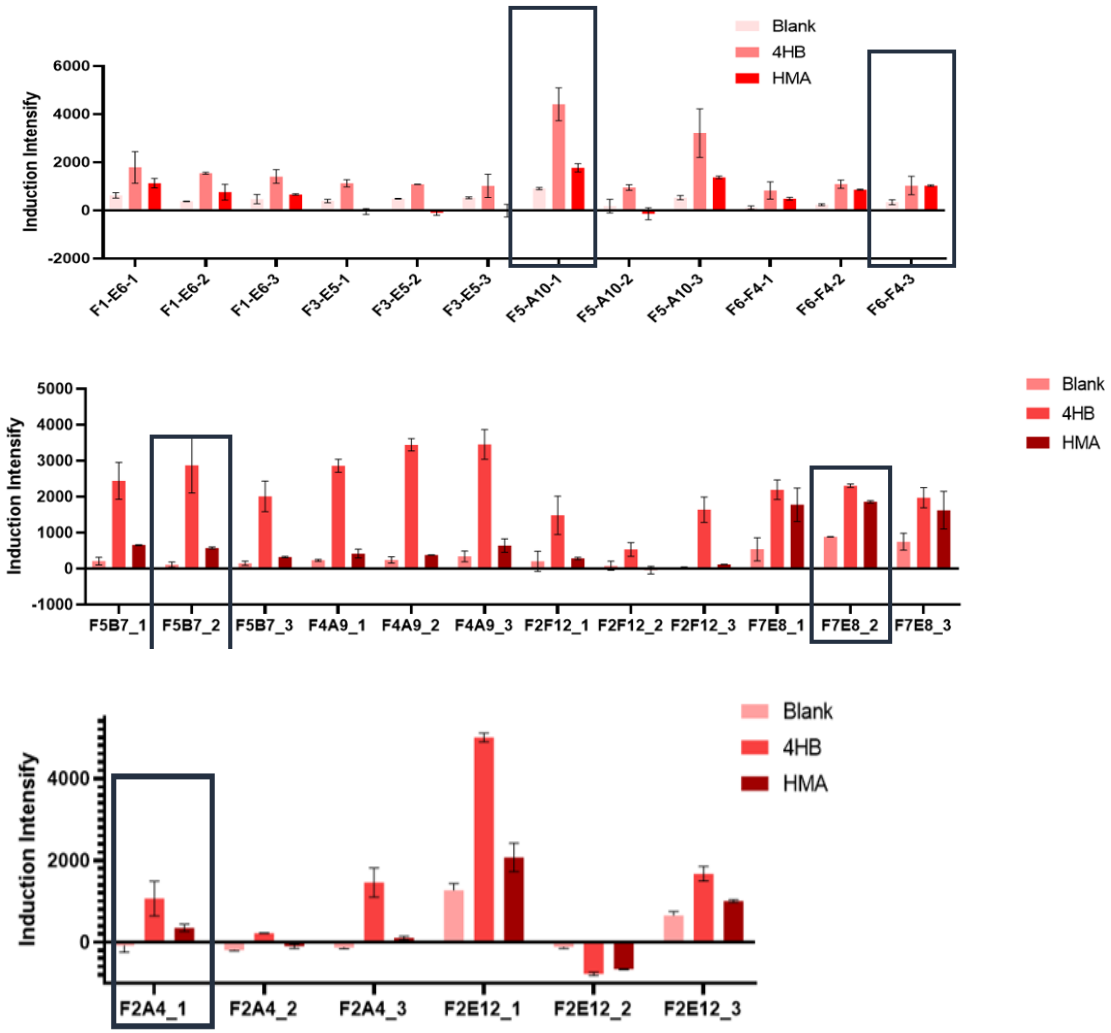

Figure 10 The induction intensity of monoclones of each clone in 10 clones

From the result we found that the HMA induction of F7-E8-3, F5-B7-2, F6-F4-3, F5-A10-1, F2-A4-1 is better. Therefore, these 5 clones were used in the further study. We used gradient HMA concentration induction assay to further study the operational Range of F7-E8-3, F5-A10-1, F6-F4-3, F5-B7-2.

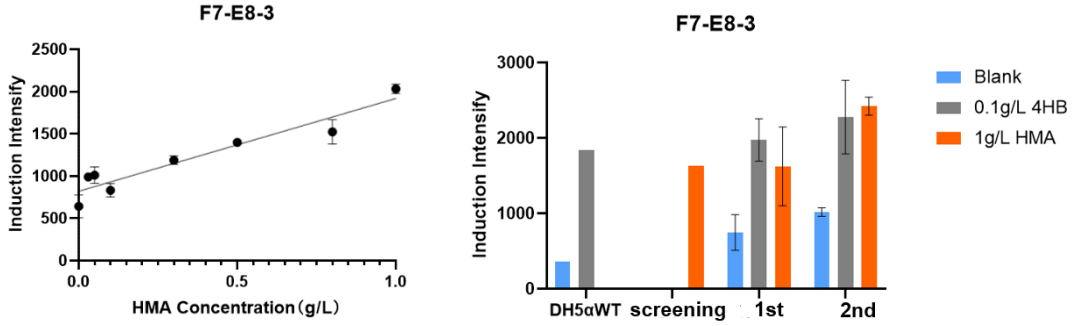

Figure 11 Left, gradient HMA concentration induction assay of F7-E8-3; right, data collection of F7-E8-3, the average value of IA/I0 = 2.3

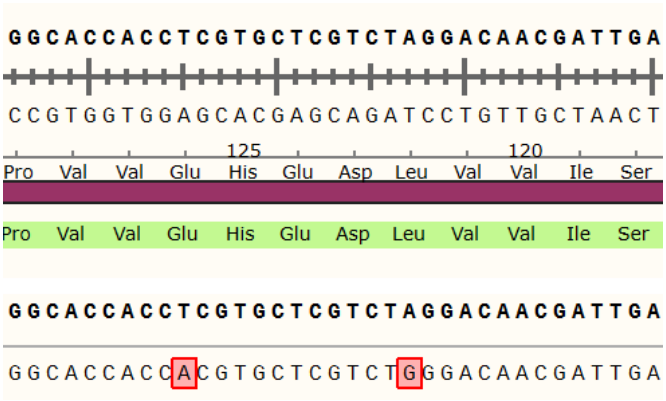

Figure 12 Sequencing of F7-E8-3

The IA of F7-E8-3 does not saturate induced by 1.0 g/L HMA. DNA sequencing showed that F7-E8-3 has 2 base substitution mutation, L123P, E126V.

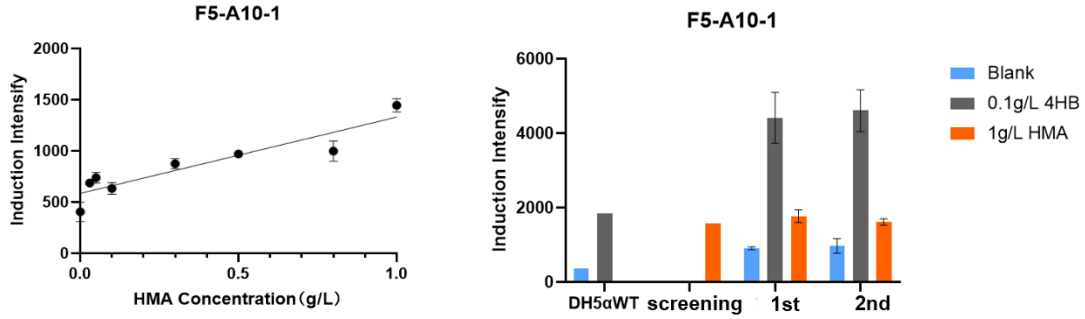

Figure 13 Left, gradient HMA concentration induction assay of F5-A10-1; right, data collection of F5-A10-1, the average value of IA/I0 = 1.7

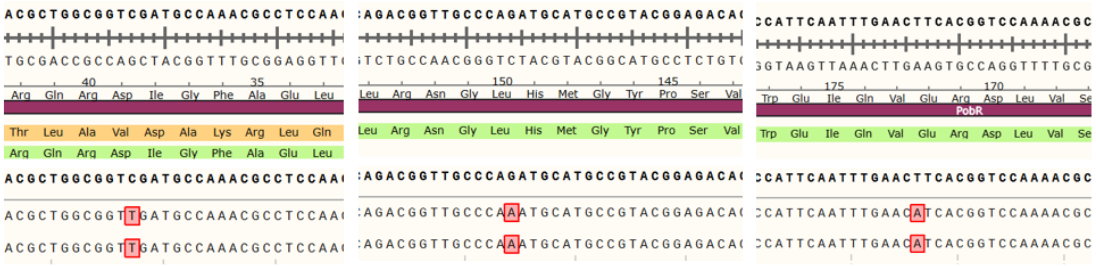

Figure 14 Sequencing of F5-A10-1

The IA of F5-A10-1 does not saturate induced by 1.0 g/L HMA. DNA sequencing showed that F5-A10-1 has 3 base substitution mutation, D39N, silent mutation at 150, E172D.

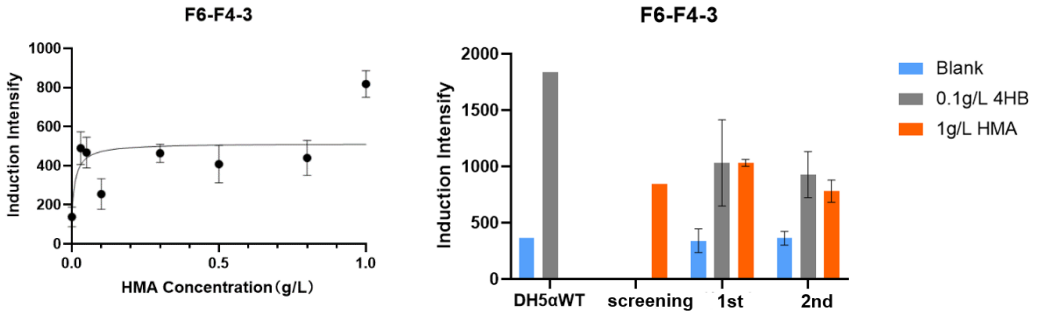

Figure 15 Left, gradient HMA concentration induction assay of F6-F4-3; right, data collection of F6-F4-3. The average value of IA/I0 = 2

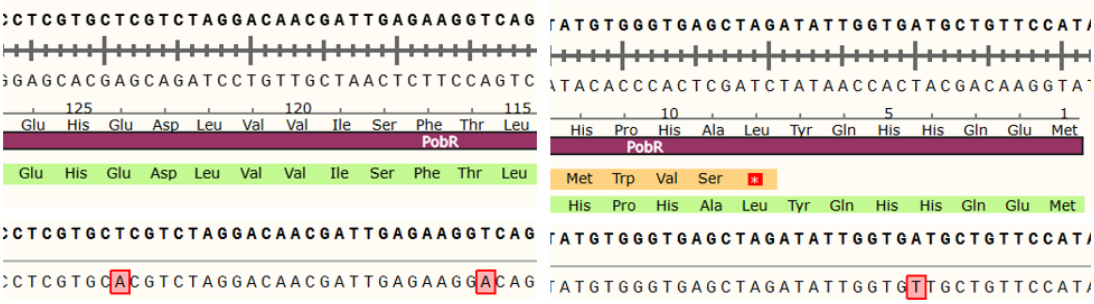

Figure 15 Sequencing of F6-F4-3

The IA of F6-F4-3 saturate induced by 1.0 g/L HMA. DNA sequencing showed that F6-F4-3 has 3 base substitution mutation, H6Q, T116S, E124V.

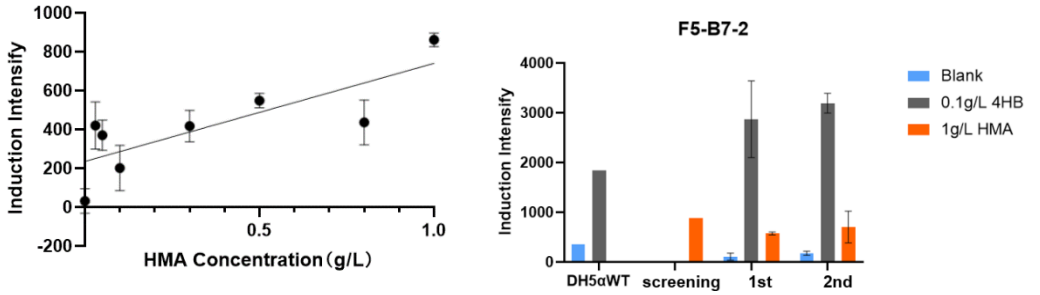

Figure 16 Left, gradient HMA concentration induction assay of F5-B7-2, right, data collection of F5-B7-2

The average value of IA/I0 = 3.8.

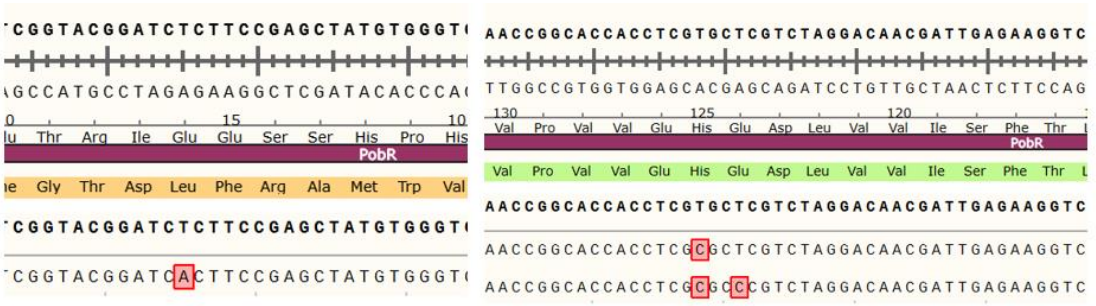

Figure 17 Sequencing of F5-B7-2

From figure 16 we found that the IA of F5-B7-2 does not saturate induced by 1.0 g/L HMA. DNA sequencing showed that F5-B7-2 has 3 base substitution mutation, E16V, E124G, H125R. The amino acid mutation sites are different from the result of docking. Therefore, we tried to construct single amino acid mutants E16V, E124G, H125R to speculate important sites for the improved induction of HMA to PobR.

8.14 Linxi Jiang

Ligand specificity test

Used HMA analogues to induce F7-E8-3, F5-A10-1, F6-F4-3, F5-B7-2 and DH5α*pobR*^{WT} to test the ligand specificity of the mutants.

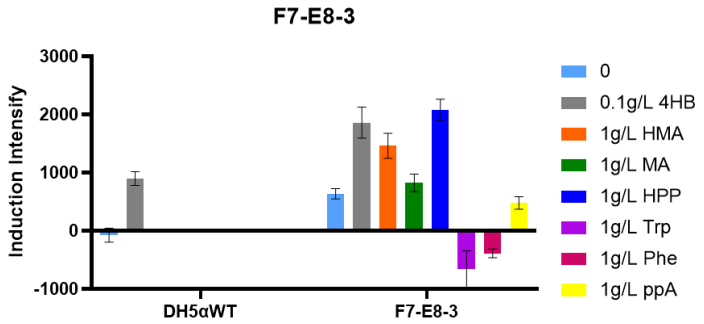

Figure 18 The induction intensity of HMA analogues to F7-E8-3

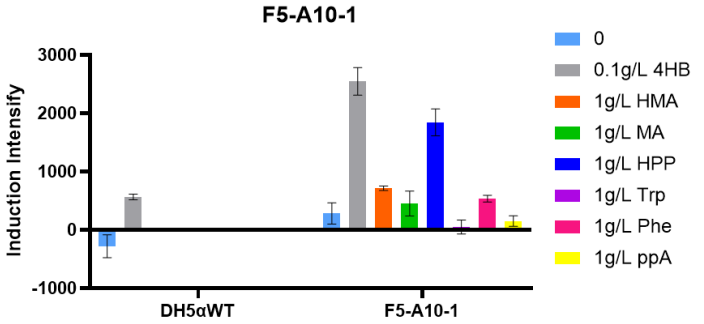

Figure 19 The induction intensity of HMA analogues to F5-A10-1

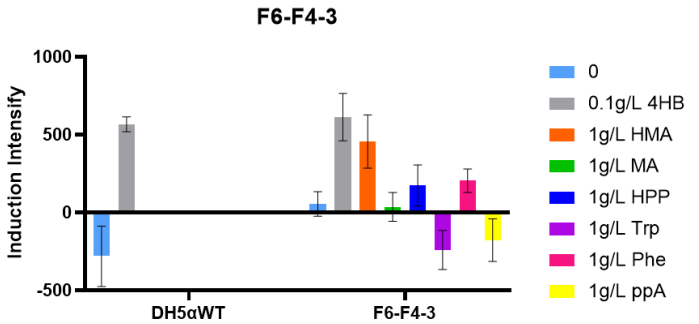

Figure 20 The induction intensity of HMA analogues to F6-F4-3

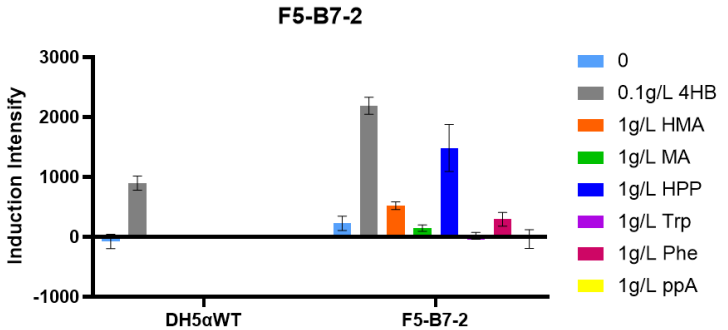

Figure 21 The induction intensity of HMA analogues to F5-B7-2

8.15 Peng Jiang

Docking between structure by RoseTTAFold and 4HB

The PobR protein structure was simulated by RoseTTAFold.

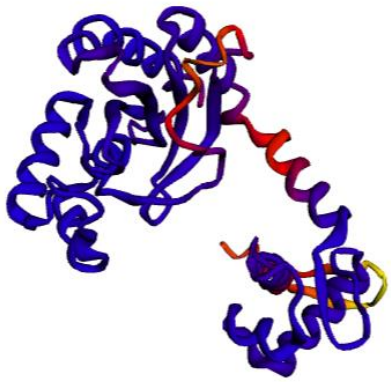

Figure 22 The protein structure simulated using RoseTTAFold

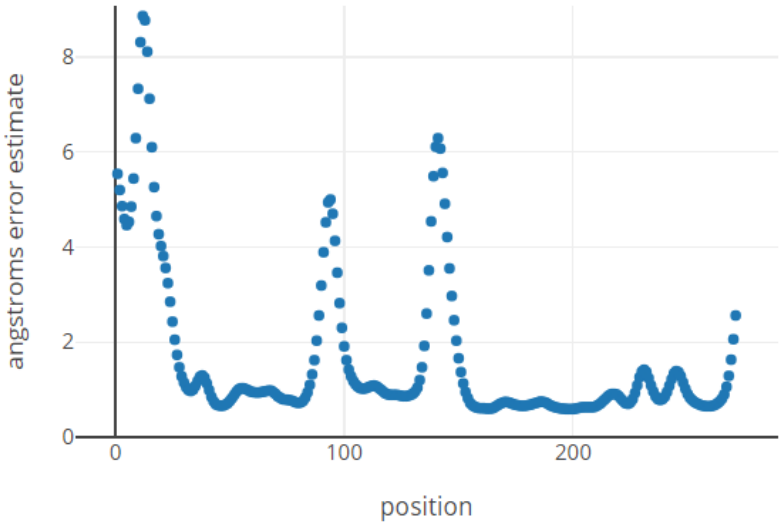

Figure 23 The predicted error of the protein structure, except for three regions

From small organic molecules Pubchem database (https://pubchem.ncbi.nlm.nih.gov/) for the chemical structure of the 4HB file, use Autodock 4.2 for semi flexible docking RoseTTAFold and 4HB. There are 70 conformations out there, the binding energy of the optimal conformation is -5.52 kcal/mol.

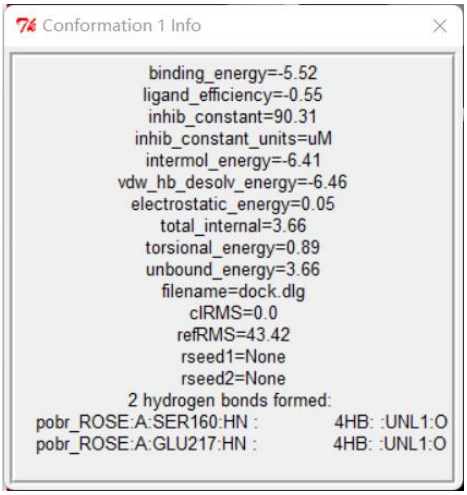

Figure 24 The parameters of this configuration by Autodock 4.2

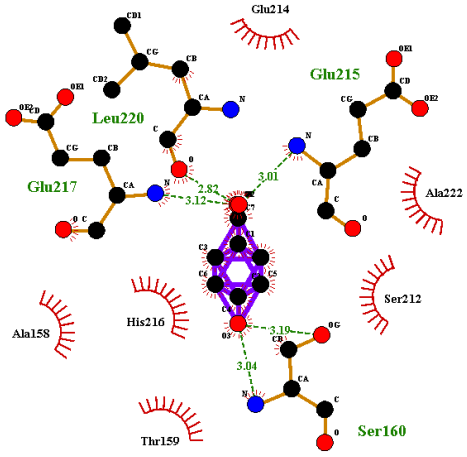

Figure 25 the interaction between the small molecule and the protein receptor in this conformation analyzed by Ligplus

As can be seen from the figure, the carboxyl side of 4HB forms hydrogen bonds with E215, E217 and L220, the hydroxyl side forms hydrogen bonds with S160, and the aromatic ring forms hydrophobic interactions with A158, T159, S212, E214, H216 and A222.

8.16 Yangjinghui Zhang

Docking between structure by AlphaFold 2 and 4HB

The protein structure of PobR was simulated using AlphaFold2, and AlphaFold2 was run through cloud computing platform (https://www.cloudam.cn/).

AlphaFold2 generated five model structures, and we selected the top-ranked model for subsequent docking, pLDDT = 91.36 (pLDDT (predicted LDDT-Cα), which is a measure of local confidence per residue in the 0~100 range. PLDDT can vary significantly along a chain, allowing the model to express high confidence in the domain, but low confidence in the linker between domains. The researchers present some evidence that regions with low pLDDT may be isolated non-structures. Regions

with pLDDT < 50 should not be interpreted, or interpreted as "possible disordered predictions".)

Autodock Vina was used to dock the model predicted by Alphafold 2 with 4HB, and the docking parameters, Vina search space coordinates were set as center_x = -0.83, center_y = -1.292, center_z = 7.229. Dimensions of search space were set as size_x = 33.75, size_y = 37.5, Dimensions of search space were set as size_x = 33.75, size_y = 37.5, size_z = 37.5. Exhaustiveness was set at 10.

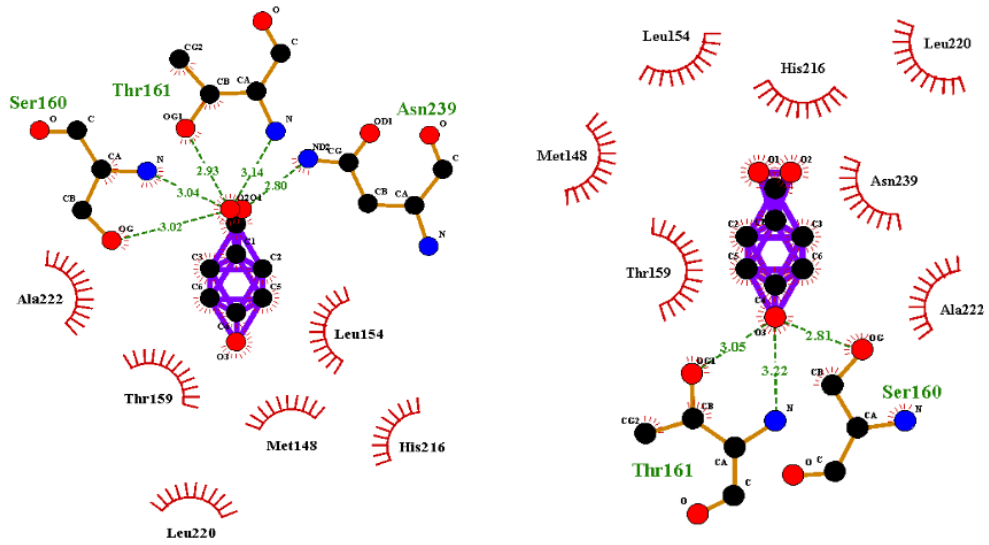

Figure 26 The top two conformations and binding energies of -6.0 kcal/mol and -6.2 kcal/mol

In Figure 26 left, the carboxyl side of benzene ring forms hydrogen bonds with S160, T161, and N239, and forms hydrophobic interactions with aromatic rings M148, T159, L154, H216, L220, and A222. In Figure 26 right, the hydroxyl side of the benzene ring forms hydrogen bonds with T161 and S160, and forms hydrophobic interactions with aromatic rings M148, L154, T159, H216, L220, A222, and N239.

It is worth noting that the two conformations are very similar, but the docking position of the small molecule ligand has changed by 180°. Therefore, it is necessary to further confirm the accuracy of the docking results.

8.16 Xinlu Liu

Site-directed mutagenesis of the PobR CDS

1. The second-round site-directed mutagenesis PCR (50 μL×3)

Reaction system:

125spm	124spm	16spm
Spm125-F: 1 μL	Spm126-F: 1 μL	Spm16-F: 1 μL
Spm125-R: 1 μL	Spm126-R: 1 μL	Spm16-R: 1 μL
PYB1a-PobR-eGFP-Cmr: 1 μL	PYB1a-PobR-eGFP-Cmr: 1 μL	PYB1a-PobR-eGFP-Cmr: 1 μL

2×HF Mix: 25 μL	2×HF Mix: 25 μL	2×HF Mix: 25 μL
DDW: 22 μL	DDW: 22 μL	DDW: 22 μL

Reaction procedure:

98℃ 5 min

98℃ 30 s
60℃ 30 s
72℃ 3 min
} ×24

72℃ 5 min

16℃ 1 h

Agarose gel electrophoresis assay showed correct bands, the concentration of the product after purified:

Spm16 (PCR): 55 ng/μL

Spm124 (PCR): 29 ng/μL

Spm125 (PCR): 29 ng/μL

2. DpnI digestion

Reaction system:

Spm125	Spm124	Spm16
DpnI: 0.2 μL	DpnI: 0.2 μL	DpnI: 0.2 μL
10×cutsmart: 1 μL	10×cutsmart: 1 μL	10×cutsmart: 1 μL
Spm125 (PCR) (29 ng/μL): 8.8 μL	Spm124 (PCR) (29 ng/μL): 8.8 μL	Spm16 (PCR) (55 ng/μL): 7.3 μL
DDW: 0	DDW: 0	DDW: 1.5 μL

8.17 Yulong Zhang

Chloramphenicol ALE pre-experiment

Transformed pYB1a-PobR$^{F5\text{-}B7\text{-}2}$-eGFP-Cmr into BL21 competent cells.

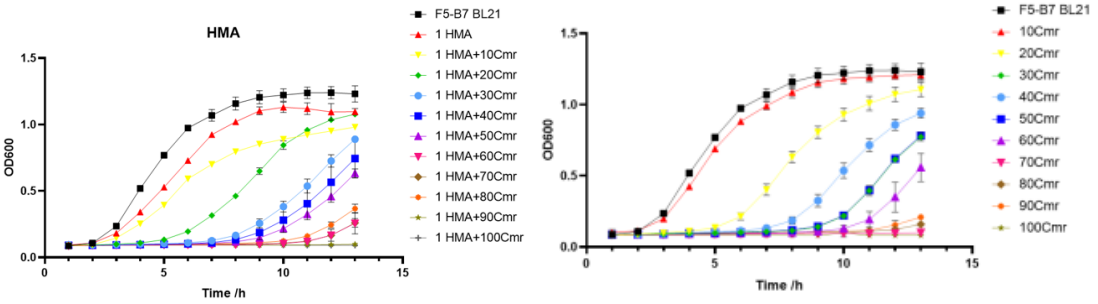

Figure 27 Growth curve of F5-B7-2 under the pressure of different concentrations of chloramphenicol, left, added 1 g/L HMA as inducer; right, no inducer

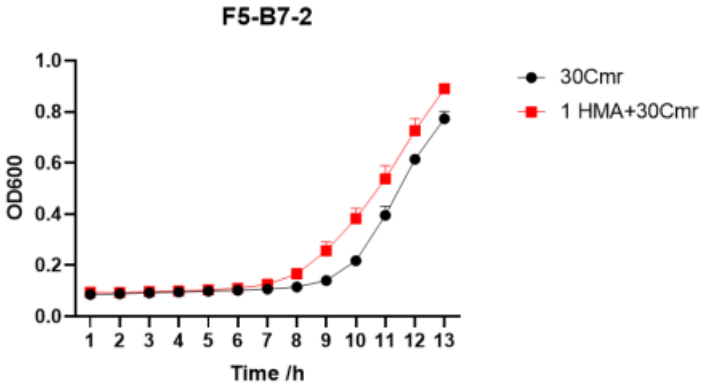

Figure 28 Comparation of the growth curve of F5-B7-2 with or without inducer under the pressure of 30 μg/mL chloramphenicol

From the figure we can see that the growth of F5-B7-2 is better from 7 h to 12 h, but the difference is tiny.

8.17 Chenhao Yang

Comparison of RoseTTAFold and AlphaFold 2

We also used protein structure simulated by RoseTTAFold to dock with the natural inducer 4HB. Coordinates Vina search space coordinates were set as center_x = -19.611, center_y =-15.137, center_z = 26.083. Dimensions of search space were set as size_x = 33.75, size_y = 37.5, size_z = 37.5. Exhaustiveness was set at 10.

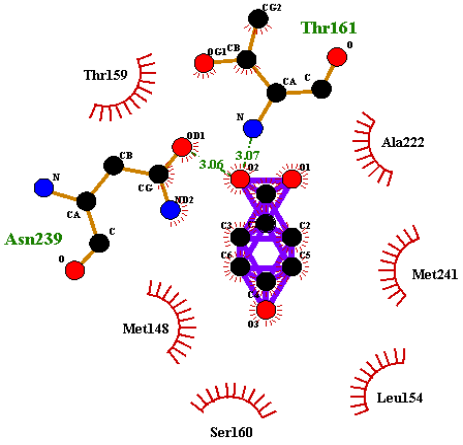

Figure 29 Schematic diagram of model by RoseTTAFold and 4HB

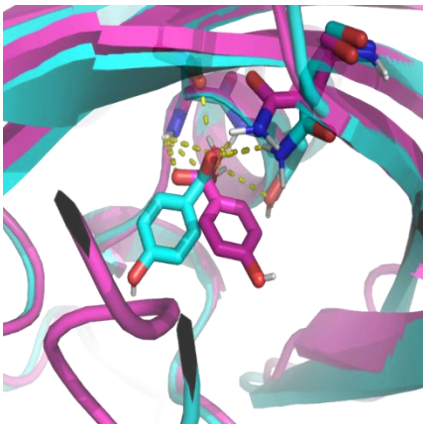

Figure 30 The cyan conformation from AlphaFold2 and the magenta conformation from RoseTTAFold

It can be seen that T161, A239 form hydrogen bonds with the carboxyl side of 4HB, and the aromatic ring forms hydrophobic interactions with M148, L154, T159, S160, A222, and M241. The comparison shows that this conformation is very similar to the first conformation of 8.16. We observe the differences between the two conformations in three dimensions. Given the similarity of ideas and the important sites mentioned in the literature, the conformation of hydrogen bonding on the carboxyl side is more plausible.

8.17 Chuyao Xu

Site-directed mutagenesis of the PobR CDS

Transformation

System:

	Spm125	Spm124	Spm16	Spm247
Competent cells	DH5α: 100 μL	DH5α: 100 μL	DH5α: 100 μL	DH5α: 100 μL
Digestion product	10 μL (255 ng)	10μL (255 ng)	10μL (401 ng)	10μL (334.4 ng)
plate	Amp50	Amp50	Amp50	Amp50

Culture at 37 ℃ for 12 h.